The relative importance of antecedent soil moisture and precipitation in flood generation in the middle and lower Yangtze River basin

Sheng Ye[1], Jin Wang[1], Qihua Ran[2]*, Xiuxiu Chen[1], Lin Liu[1]

[1] Institute of Hydrology and Water Resources, School of Civil Engineering, Zhejiang University, Hangzhou 310058, China

[2] State Key Laboratory of Hydrology-Water Resources and Hydraulic Engineering, Hohai University, Nanjing 210098, China

* Corresponding author: Qihua Ran

Email address of the corresponding author: ranqihua@zju.edu.cn

April 21, 2022

Abstract

Floods have caused severe environmental and social economic losses worldwide in human history, and are projected to exacerbate due to climate change. Many floods are caused by heavy rainfall with highly saturated soil, however, the relative importance of rainfall and antecedent soil moisture and how it changes from place to place has not been fully understood. Here we examined annual floods from more than 200 hydrological stations in the middle and lower Yangtze River basin. Our results indicate that the dominant factor of flood generation shifts from rainfall to antecedent soil moisture with the increase of watershed area. The ratio of the relative importance of antecedent soil moisture and daily rainfall (SPR) is positively correlated with topographic wetness index and has a negative correlation with the magnitude of annual floods. This linkage between watershed characteristics that are easy to measure and the dominant flood generation mechanism provides a framework to quantitatively estimate potential flood risk in ungauged watersheds in the middle and lower Yangtze River basin.

Key words: flood generation, scaling effect, topographic wetness index

1. Introduction

Flooding is one of the most destructive and costly natural hazards in the world, resulting in considerable fatalities and property losses (Suresh et al., 2013). River floods have affected nearly 2.5 billion people between 1994 and 2013 worldwide (CRED, 2015), and caused 104 billion dollars losses every year (Desai et al 2015). The damages may be further exacerbated by increasing frequency and intensity of extreme rainfall events according to climate change projection (IPCC 2012; Ohmura and Wild 2002). Flood control infrastructures and more accurate predictions are needed to reduce flood damages, which requires better understanding of the underlying mechanism of flood generation as well as the drivers of change (Villarini & Wasko 2021).

Numerous studies have been conducted to investigate the cause of floods across the world (Bloschl et al 2013; Munoz et al 2018; Zhang et al 2018). Many studies focused on examining the environmental and social characteristics that lead to specific catastrophic flood events (Bloschl et al 2013; Liu et al 2020; Zhang et al., 2018). Others concentrated on single locations, usually catchment outlets, to explore the influential factors of floods and the future trends (Brunner et al., 2016; Munoz et al 2018). Yet given the amount of data and time required, it is not practical to apply these detailed studies to hundreds of catchments to generate an overview of the flood generation mechanism at large scale.

Recently, researchers started to investigate the dominant flood generation mechanisms at regional scales (Berghuijs et al 2019b; Do et al 2020; Garg & Mishra 2019; Smith et al 2018; Tramblay et al 2021; Ye et al 2017). Most of these studies are conducted in North America and Europe with well-documented long-term records (Berghuijs et al 2016; Bloschl et al 2019; Do et al 2020; Musselman et al 2018; Rottler

et al 2020). Such researches were just conducted in China recently, though still limited (Yang et al 2019; Yang et al 2020).

As the largest river in China, Yangtze River basin has long suffered from floods. In summer 2020, 378 tributaries of the Yangtze River had floods exceeding the alarm level, causing billions of dollars damage (Xia et al., 2021). With the increasing public awareness, more accurate prediction is needed, which relies on better understanding. However, due to the limitation of observations, there are only a few regional studies of the flood generation mechanism in China, even little in the Yangtze River basin (Zhang et al 2018; Yang et al 2019; Yang et al 2020). The large number of dams and reservoirs built along the river further complicated the situation (Feng et al., 2017; Qian et al 2011; Yang et al 2019).

Because of the relatively warm temperature, snowmelt has little impact on flood generation in the Yangtze River basin (Yang et al 2020). Floods in the Yangtze River basin usually occur during summer with relatively wet soil and high rainfall (Wang et al 2021). Heavy rainfall with high antecedent soil moisture has also been identified as dominant driver of floods across world (Beighuijs et al 2019b; Garg et al 2019; Tramblay et al 2021; Wasko et al 2020). Recently, studies started to examines the relative importance of rainfall and antecedent soil moisture in flood generation (Brunner et al., 2021; Wasko et al., 2021; Bennett et al., 2018; Bertola et al., 2021). Quantitative evaluation of the relative contribution of rainfall and antecedent soil moisture and its change across watersheds is still limited and currently unavailable in China (Liu et al., 2021; Wu et al., 2015).

Based on the watersheds in the middle and lower Yangtze River basin, this study attempts to explore the following questions: 1) is there a way to quantitatively describe

the relative importance of antecedent soil moisture and rainfall on flood generation; and 2) how would this combination of flood-generation rainfall and soil moisture vary across watersheds, and what are the influential factors. Based on the observations and model estimation (Section 2), the spatial distribution patterns of antecedent soil moisture and rainfall were obtained and analyzed to investigate their individual contribution to flood generation and the influential factors (Section3). This allows for further examination of the relative importance of antecedent soil moisture and rainfall on flood generation and its linkage to watershed characteristics as well as its implications to flood prediction (Section 4), all the results are summarized in Section 5.

2 Methods

2.1 Study area

The Yangtze River is the largest river in China, with a total length of 6,300 kilometers and annual discharge of 920km^3 at the outlet (Yang et al., 2018). It drains through an area of 1.8*10^6 km^2, lying between 90°33'and 122°25'E and 24°30'and 35°45'N, and is home to over 400 million people, most of which live in the middle and lower Yangtze River basin (YZRB) (Cai et al., 2020). The elevation of the YZRB declines from west to east: from over 3000m in Qinghai-Tibet Plateau, to around 1000m in the central mountain region, and the 100m in Eastern China Plain (Wang et al., 2013). The vegetation types in the YZRB are forests, shrubs, grassland and agricultural land, accounting for 11.85%, 12.65%, 32.26% and 42.88% respectively. Grassland and shrubs are the dominant vegetation in the middle and upper YZRB, while the downstream YZRB is dominated by forests and agricultural land (Miao et al., 2010). There are more than 51,000 reservoirs of different sizes in the whole basin, including 280 large ones (Peng et al., 2020).

Most of the YZRB is semi-humid and humid, with a typical subtropical monsoon climate. The mean annual temperature is approximately 13.0 ℃, varying from −4 ℃ to 18℃ downstream. The mean annual precipitation of the whole basin is about 1200 mm, increasing from 300mm in the western headwaters to 2400 mm downstream. (Li et al., 2021). Most of the precipitation comes between June and September, the premise of persistent heavy rain in the Yangtze River basin is the frequent activity of weak cold air in the north (Tao et al., 1980) and the intersection of mid-latitude air mass and monsoon air mass (Kato et al., 1985). Studies have found that both annual precipitation and the frequency of extreme precipitation events have increased in the middle and lower reaches of the Yangtze River (Qian et al., 2020; Fu et al., 2013). As a result, floods have occurred frequently in the middle and lower reaches of the Yangtze River, where most of the population in the YZRB live (Liu et al., 2018).

2.2 Data

In this work, we focus on the middle and lower reaches of the Yangtze River for the high population density and increasing flood risk. The 30-meter digital elevation model (DEM) was downloaded from Geospatial Data Cloud (http://www.gscloud.cn/), from which the drainage area corresponding to the hydrological station was extracted by ArcGIS. Daily precipitation data and temperature data between 1970 and 2016 from 247 meteorological stations within and near the YZRB were downloaded from China Meteorological Data Network (https://data.cma.cn/) (Figure 1). The temperature data was used to estimate potential evaporation. The observed precipitation and estimated potential evaporation were interpolated into the whole YZRB using Thiessen polygon method (Meena et al., 2013). The interpolated precipitation and potential evaporation were then averaged for the drainage area corresponding to each hydrological station.

The daily streamflow data was collected from 267 hydrological stations from Annual Hydrological Report of the People's Republic of China. Among which, 224 stations with at least 20 years records from both the period from 1970 to 1990 and the period from 2007 to 2016 were selected (see Figure S1 for data availability). Information of 361 reservoirs in the middle and lower YZRB, including capacity and controlling area was downloaded and extracted from the Global Reservoir and Dam database (GRanD) (Lehner et al 2011). Previous study showed that this database provides reliable information of middle and large reservoirs in China (Yang et al 2021). Watersheds with more than 80% of the drainage area under control reservoirs according to GRanD database and/or located right downstream of reservoirs and water gates were considered as watersheds under strong regulation (regulated watersheds).

2.3 Calculation of hydrological and topographic characteristics

Potential evaporation estimation

The temperature data was used to estimate potential evaporation following the Hargreaves method (Allen et al., 1998; Vicente et al., 2014; Berti et al., 2014).

$$ET_0 = 0.0023 \times (Tmax - Tmin)^{0.5} \times (Tmean + 17.8) \times Ra \quad (1)$$

where ET_0 is potential evaporation (mm/d), *Tmax* is the highest temperature (°C), *Tmin* is the lowest temperature (°C), *Tmean* is the mean temperature (°C), and *Ra* is the outer space radiation [MJ/(m^2·d)], which can be calculated as follows:

$$Ra = 37.6 \times d_r \times (\omega_s \sin\varphi \sin\delta + \cos\varphi \cos\delta \sin\omega_s), \quad (2)$$

where d_r is the reciprocal of the relative distance between the sun and the earth, ω_s is the angle of sunshine hours, δ is the inclination of the sun (rad), φ is geographic

latitude (rad). d_r, δ and ω_s can be calculated by the following formula:

$$d_r = 1 + 0.033 \times \cos\left(\frac{2\pi J}{365}\right), \quad (3)$$

$$\delta = 0.409 \times \sin\left(\frac{2\pi J}{365} - 1.39\right), \quad (4)$$

$$\omega_S = \arccos(-\tan\varphi \tan\delta) \ , \quad (5)$$

where J is the daily ordinal number (January 1st is 1).

Soil water storage estimation

The soil water storage was estimated based on the daily water balance (Berhuijs et al., 2016, 2019):

$$\frac{\mathrm{d}S}{\mathrm{d}t} = P - ET - \max(Q, 0), \quad (6)$$

Where S is the soil water storage (mm), which is initially set to 0. Due to the long term of simulation, the change of initial value wouldn't significantly affect the results. P is precipitation (mm/d), Q is discharge normalized by area (mm/d), ET is evaporation (mm/d), which can be calculated from potential evapotranspiration (ET_0), where the soil water storage (S) is used as the upper limit of daily ET:

$$ET = \min(0.75 \times ET_0, \mathrm{S}), \quad (7)$$

The estimation of soil water storage and ET are highly simplified and is not used for prediction but to capture the first order of the seasonal variation and to help develop a framework that differentiates the relative contribution of precipitation and soil moisture in flood generation.

Topographic wetness index estimation

Topographic wetness index was calculated to represent the combined impacts of drainage area and topographic gradient (Alfonso et al., 2011; Grabs et al., 2009):

$$TWI = \ln(A_d/\tan\alpha), \quad (8)$$

where A_d is drainage area and α is topographic gradient estimated from DEM. TWI represents the propensity of subsurface flow accumulation and frequency of saturated conditions, thus can be used to predict relative surface wetness and hydrological responses (Meles et al 2020). It is widely used to quantify topographic impact on hydrological processes (i.e., spatial scale effects, hydrological flow path, etc.), as well as in land surface models for hydrological, biogeochemical and ecological processes (Sorensen et al 2006).

2.4 Quantification of the relative importance of soil moisture and precipitation during floods

The maximum daily discharge of each year was selected as annual flood, which was then averaged across years as the mean annual maximum flood (AMF). The observed rainfall on that day and the estimated soil water storage at the day before were also averaged across years as daily rainfall (P) and antecedent soil moisture (S_0). Since almost all the AMFs in our study region come during rainy season when rainfall comes in most of the days. To avoid the bias that may be caused in event separation, the soil moisture at the day before AMF was used as antecedent soil moisture, instead of the day before the event of AMF. To examine the impacts from long-lasting rainfall event, especially for the large watersheds with longer concentration time, we also calculated the mean accumulated rainfall from two days (rainfall on the flood day and the day

197 before, P_2) to seven days (weekly rainfall, P_7).

198 The percentile of antecedent soil moisture (S_0) was calculated to represent the
199 relative saturation of soil moisture in the time series; while the percentile of daily
200 rainfall (P) was estimated to show the relative intensity (P'), representing the relative
201 magnitude of rainfall in flood generation. The percentile of accumulated rainfall was
202 also calculated for the two-day to seven-day rainfall.

203 To quantify the relative importance of antecedent soil moisture and rainfall in flood
204 generation, the ratio between these two factors at the AMFs was derived: SPR = S'/P'.
205 When SPR is large, the antecedent soil moisture is much closer to the maximum, while
206 the daily rainfall is less extreme, floods are more affected by the antecedent soil
207 moisture. On the other hand, a smaller SPR indicates relatively larger magnitude of
208 rainfall comparing with antecedent soil moisture, that is, rainfall is more extreme and
209 influential in flood generation.

210 **3 Results**

211 **3.1 Spatial patterns of antecedent soil moisture and precipitation during floods**

212 Figure 2 shows the spatial distribution of the percentile of antecedent soil moisture and
213 daily rainfall during the annual maximum floods (AMFs) in the middle and lower
214 reaches of the Yangtze River. As we can see from Figure 2a, in the middle and lower
215 reaches of YZRB, when AMFs occurred, the percentile of antecedent soil saturation
216 was generally high, most of them are larger than 0.6: the farther away from the main
217 stream, the more saturated the soil was. On the other hand, along and near the main
218 stream and the delta, the antecedent soil saturation rate could be much smaller, even
219 less than 0.4.

Figure 2b shows the daily rainfall during the AMFs. As we can see, the percentile of daily rainfall is relatively high (>0.8) at more than half of the study sites, while it is small (<0.5) for the sites along the main stream and in the delta (Figure 2b). Comparison between Figure 2a and b suggests that, except the sites on the main stream and in the delta, sites with relatively high antecedent soil saturation rate (i.e., >0.8, the blue dots) during AMFs are also the ones with relatively small daily rainfall contribution (i.e., <0.8, the light blue and cyan dots). That is, for these sites, the AMFs are usually occurring at a near saturated soil condition while extreme rainfall at flood day is not necessary, suggesting the relative importance of soil saturation rate. For the sites with both the percentile of soil moisture and rainfall between 0.6 and 1, both the antecedent soil moisture and rainfall play important roles in flood generation. As for the sites on the main stream and in the delta, both antecedent soil moisture and rainfall are low during AMFs, this is likely due to the regulations from large reservoirs and water gates.

3.2 The scaling effect in the contribution of antecedent soil moisture and rainfall

To further investigate the relative importance of antecedent soil moisture and rainfall in flood generation and the potential influential factors, we examined their correlation with catchment area (Figure 3). Given the complicated environmental and social impacts, the regulated watersheds and sites on the main stream are presented separately (the green dots and cyan dots in Figure 3 respectively). Our study will focus on the sites that are not dominated by regulation (the blue dots in Figure 3), for simplicity, we will refer them as natural watersheds.

As we can see from Figure 3, during the occurrence of AMFs, the percentile of antecedent soil saturation increases with watershed area (p-value<0.001), while the percentile of daily rainfall decreases with watershed area (p-value<0.001). That is, with

the increase of watershed size, antecedent soil moisture becomes more and more saturated while the precipitation is less and less extreme during AMFs; suggesting the rising contribution of antecedent soil moisture and declining importance of daily precipitation in flood generation. As for the regulated watersheds (green dots in Figure 3), there is no clear correlation between drainage area and the percentile of antecedent soil moisture or rainfall, which is understandable. Meanwhile, both the percentile of antecedent soil moisture and rainfall decreases with watershed area for main stream sites.

3.3 The scaling impacts on accumulated rainfall

The saturation of soil before floods could be due to previous rainfall events, and could also be caused by accumulated rainfall in long-lasting rainfall events that eventually generate floods (Xie et al., 2018). Figure 4 presents the correlation between the percentile of accumulated rainfall and drainage area. When single day rainfall is considered, it is negatively correlated with drainage area (Figure 3a); when accumulated rainfall is considered, the correlation gradually shifts from negative to positive correlation (Figure 4). For example, when two-day rainfall was examined, the correlation between accumulated rainfall and drainage area shifts from negative to positive at 10,000 km^2; the negative correlation in Figure 3a is only valid for watersheds larger than 10,000 km^2 (Figure 4a). This transition area increases from 10,000 km^2 for two-day rainfall to 100,000 km^2 for four-day rainfall (Figure 4c). The number of watersheds with negative correlation also decreases. Eventually, the weekly rainfall has similar positive correlation with drainage area like antecedent soil moisture (Figure 4f). The increase of transition area may be explained by the increasing response time and confluence time in large watersheds: it takes days to generate flow events by heavy

rainfall and for them to reach outlets where it can be observed in large watersheds. This is also consistent with the conclusion in the Yellow River Basin (Ran et al., 2020) and our previous findings of the dominant flood generation mechanism in the middle and lower YZRB: weekly rainfall is the dominant flood driver for sites on the main streams and the major tributaries (Wang et al 2021). The regulated watersheds don't show significant correlation which is understandable for the strong human intervention. For the negative correlation between accumulated rainfall and drainage area at main stream sites, it is difficult to decide whether it is due to scaling effect or human intervention.

3.4 The interlink of watershed characteristics, flood, antecedent soil moisture and rainfall

Figure 5 presents the percentile of antecedent soil moisture and rainfall during the AMFs at the study watersheds, the circles are scaled by watershed size and colored with topographic gradient. Except the watersheds with strong human intervention (regulated ones and the ones on main stream), there is a negative correlation between the contribution of rainfall and antecedent soil moisture. The lower right of the scatter are mostly big blue dots, which are large watersheds with gentle topographic gradient. That is, AMFs usually occur when soil moisture is close to saturation while extreme rainfall is not necessary for AMFs in these watersheds. On top of the scatter are relatively small yellow and green dots, those are medium to small watersheds with steep topographic gradient. That is, AMFs are usually generated with extreme rainfall, while the saturation of soil moisture is not necessary. This negative correlation indicates the shift of dominance in AMFs generation from extreme rainfall to antecedent soil saturation from small steep watersheds to large flat ones.

Figure 6 shows the relative importance of antecedent soil moisture and rainfall. For

292 the natural watersheds (the circles), SPR increases with drainage area and declines with
293 topographic gradient. That is, the larger the drainage area is, the more essential the
294 contribution of antecedent soil moisture to floods is, and the less influential rainfall is
295 in flood generation. For watersheds with similar drainage area (i.e., the green or light
296 blue dots in Figure 6b), topographic gradient also cast impacts on SPR: SPR decreases
297 with slope. That is, the relative importance of rainfall increases at steeper watersheds.
298 This may be attributed to the shortened hydrological response time due to the steep
299 topography which facilitates rainfall induced floods generation. As a combination of
300 both drainage area and topographic gradient, TWI is positively correlated with SPR at
301 natural watersheds, with less scatter than the correlation between SPR and drainage
302 area or topographic gradient alone. That is, watersheds with larger area and gentler
303 topographic gradient that are easier to get wet tend to have larger SPR: soil saturation
304 is more important in flood generation. There is no significant correlation between SPR
305 and TWI for the regulated watersheds along tributaries (black triangles). However, the
306 sites on main stream show opposite pattern: the SPR at these sites decreases with TWI
307 and drainage area. It is difficult to determine whether this is because of reservoir
308 regulation or not. More data about watersheds larger than 10,000km^2 but with limited
309 human intervention are needed to examine this hypothesis.

310 Besides TWI, SPR is also correlated with the magnitude of AMF (Figure 7). As
311 Figure 7 shows, the area normalized flood peak declines with flood-generation SPR.
312 Watersheds with large flood peak are mostly the ones with steep topographic gradient
313 and small SPR (i.e., SPR<1) and *vice versa*. Similar correlation was also found at event
314 scale in our experimental mountainous watershed, which locates at a headwater of
315 Yangtze River (Liu et al 2021).

4 Discussion

4.1 The relative importance of antecedent soil moisture and rainfall in flood generation

While soil moisture and rainfall are the two main drivers of floods in the middle and lower Yangtze River basin, the dominance of each factor varies across the relatively natural watersheds. Floods in large watersheds are usually generated when soil is almost saturated despite of the relatively small rainfall amount, while extreme rainfall is usually observed during floods in small to medium watersheds (blue dots in Figure 3). The rising contribution of antecedent soil moisture in large watersheds was consistent with the findings in Australian watersheds (Wasko & Nathan, 2019); and the declining influence of rainfall at larger watersheds was also found in Indian watersheds (Garg et al 2019). This contrast correlation with watershed size indicates a shift of dominance in AMFs generation, which may be attributed to the longer confluence time in the large watersheds and less heterogeneity in small watersheds.

This shift of dominance can be observed more straightforward from the negative correlation between the percentile of rainfall and antecedent soil moisture in Figure 5. The natural watersheds in Figure 5 could be grouped into three classes based on their drainage area and topographic gradient. When a watershed is large and flat, flood occurrence is mainly determined by soil saturation (i.e., the big blue dots at the lower right of the scatter); on the other hand, when a watershed is small and steep, heavy rainfall takes over the dominance (i.e., the small yellow and green dots at the upper left of the scatter). Between these two groups are relatively small watersheds with gentle topographic gradient, where the occurrence of AMF requires both highly saturated soil and relatively heavy rainfall. That is, the dominant influential factor(s) in AMFs

generation across watersheds is correlated with the topographic characteristics (i.e., watershed size and topographic gradient). This helps quantify the relative importance of soil moisture and rainfall in flood generation in the existing work.

This shift of dominance is not observed in the main stream sites (i.e., cyan dots in Figure 3), where the percentile of both antecedent soil moisture and precipitation declines with drainage area. This may be attributed to the more complicated flood generation mechanism at large scale as well as the strong human intervention on main stream (e.g., reservoirs, water gates regulation, etc.) (Gao et al., 2018; Long et al., 2020; Zhang et al., 2017). The major responsibilities of reservoirs on the main stream are to reduce peak flow and postpone the time to flood peak (Volpi et al., 2018). As a result, the original flood peak would be delayed by regulation and the actual flood peak would occur when rainfall declines/stops and soil water drains. Another possibility is that when watershed size is larger than 100,000km^2, the impact of antecedent soil moisture declines as well. To examine this hypothesis, more data from watersheds larger than 100,000km^2 and with limited human intervention is needed. However, this is above the scope of this work and requires future studies.

4.2 Linkage between topographic characteristics, SPR and floods

The correlation between TWI and SPR (Figure 6c) demonstrates that the relative importance of soil moisture and rainfall could be inferred from topographic characteristics quantitatively. We could derive the relative dominance of soil moisture and rainfall in flood generation in specific watershed from its TWI for the natural watersheds without significant human intervention. Rainfall and soil moisture level have been identified as dominant drivers of floods, individually or together, in watersheds worldwide (Berghuijs et al 2016, 2019b; Garg & Mishra 2019; Tramblay et

al 2021; Ye et al 2017). Our findings provide a framework to quantify the relative importance of rainfall and soil moisture and to further identify the influential factors of their importance based on topographic characteristics that are easy to measure.

Meanwhile, the SPR also present a negative correlation with the magnitude of AMFs (Figure 7). That is, we could infer the mean annual AMF based on SPR for each watershed. Since the characteristic SPR could be estimated from TWI, we could derive quantitative estimation of the mean AMFs from topographic characteristics that are easy to measure, even in watersheds with little hydrologic records. This would be helpful for flood control management in ungauged watersheds, especially in the mountainous watersheds with risks of flash floods. Similar correlation was also found in the observations from our experimental watershed, a headwater of Yangtze River (Liu et al 2021). The ratio of observed antecedent soil moisture and event precipitation also presents similar decline trend with discharge at event scale. However, the correlation between SPR and discharge at event scale is preliminary, more data with higher resolution and detailed analysis are needed for validation at event scale. For this study, our goal is to present the framework to derive flood generation SPR that could be estimated from topographic characteristics and to provide information of mean AMFs.

In conclusion, based on the topographic characteristics, we could derive the relative importance of soil moisture and rainfall in flood generation (SPR); and from this relative importance ratio, we could further infer the average flood magnitude at these watersheds. As a result, we could link the topographic characteristics and annual floods through the characteristic SPR during the AMFs.

4.3 Implications

Our findings could be helpful for potential flood risk evaluation in ungauged basins, e.g., headwaters in the mountainous region. With the construction of large reservoirs, the capability of flood risk control has improved substantially along main stream (Zou et al., 2011; Zhang et al., 2015). However, it is still difficult for quantitative evaluation of flood risk in upstream mountainous watersheds, which are vulnerable to floods but difficult for hydrological modeling and prediction due to little hydrologic records.

Our findings suggest that we could derive the flood-generation SPR of each watershed from drainage area and topographic gradient that are easy to measure. The correlation between SPR and flood peak provides information of the mean annual floods in ungauged watersheds. Therefore, in regions without observation data, to build flood control infrastructure such as dams and gates, the mean annual flood peak obtained by SPR based on the topographic characteristics can be used to provide quantitative information for flood control and disaster management. Flood control infrastructures could be designed based on the estimated mean annual flood peak as well as the demographic information. With further validation of this framework at event scale, by using the observed soil moisture from remote sensing data and precipitation forecast to generate real-time prediction of SPR values, we could further provide early warning of floods in these ungauged watersheds. But this needs more data and examination in future studies.

4.4 Limitations

Previous works usually identify the dominant flood generation mechanism based on the comparison of the timing of events (Berghuijs et al 2016; 2019b; Bloschl et al 2017; Ye et al 2017). Similar work has been implemented in our study watersheds, suggesting the importance of soil moisture and rainfall (Wang et al 2021). Based on that, we further

looked into the records to quantitatively evaluate the relative importance of soil moisture and rainfall in flood generation. However, there are limitations in our methods.

The precipitation data we used were averaged for the study watersheds from 247 meteorological stations. Given the large area and considerable spatial heterogeneity, the precipitation data we used may not always be representative of the actual precipitation events. The daily data could also average the rainfall intensity at hourly scale, which could be influential in small mountainous watersheds. ET was scaled as $0.75*ET_0$ to make sure it is smaller than the potential evaporation. This is a simplified estimation of ET; more sophisticated method is needed in further analysis on specific catchments at event scale.

The estimation of soil moisture is also highly simplified, which cannot be considered as precise estimation at event scale. To reduce the influence from this simplification, we used the percentile of soil moisture to represent the relative saturation of soil moisture as well as the seasonal trend of soil moisture, which was then compared with the percentile of rainfall. While more sophisticated models can be used for soil moisture estimation, there could still be substantial uncertainties (Zaherpour et al., 2018; Ran et al 2020). Yet the seasonal trend and the relative magnitude, after averaging through long-term records would be less impacted by the simplification in estimation (Berghuijs et al 2019; Zhang et al 2019).

It is possible that soil moisture at the day before the AMFs may not be the soil moisture before event in large catchments due to the long concentration time. We estimated the concentration time for 10 sites with largest drainage area (larger than 100,000 km²): the ones on the main stream and at the outlets of major tributaries following the USBR method (USBR 1973; Gericke & Smithers 2014). The

concentration time is mostly within two days for main stream sites and is less than 24hr for sites at the outlets of major tributaries (Table S1). Since the rest of the sites are all smaller than these ones, so would be the concentration time. That is, for the natural watersheds we focused on, the concentration time is likely to be within one day. Thus, the soil moisture at the day before AMFs would contribute to the generation of AMFs, and should be applicable for this study.

Besides, the exchange with groundwater was not considered in the soil moisture estimation. The exchange with groundwater is more complicated and heterogenous (i.e., rivers could receive groundwater recharge in hilly area and recharge groundwater in lower land (Che et al 2021)). According to Huang et al. (2021), the variation of groundwater level in the Yangtze River basin is relatively small. Since the goal of this study is to capture the first order seasonal variation of soil moisture and develop a framework that differentiates the relative importance of precipitation and soil moisture in flood generation, in this study, we estimated the soil moisture following Berhuijs (et al 2016, 2019) with a simple water balance equation.

Moreover, this work is focused on the relative importance soil moisture and rainfall, the impact of snowmelt is not considered due to the warm and humid climate in the study watersheds. To apply our findings to cold watersheds with significant impact of snow, the snowmelt component needs to be incorporated. In addition, our method is based on the average values from many years. While previous work indicated that the occurrence of floods in our study watersheds are highly concentrated (Wang et al 2021), there could be strong inter-annual variability in other watersheds. In future studies, annual scale and event scale analysis are needed to examine and improve our findings before it can be applied to watersheds with more diverse climate and landscape

conditions. more comprehensive models with sophisticated groundwater component, remote sensing data, and reanalysis product with higher spatial-temporal resolution are needed to provide more accurate estimation of soil moisture, ET, and refine the estimation of the flood-generation SPR.

5 Conclusions

Heavy rainfall on highly saturated soil was identified as the dominant flood generation mechanism across world (Berghuijs et al 2019; Wang et al 2021; Wasko et al 2020). This study aims to further evaluate the relative importance of antecedent soil moisture and rainfall on floods generation and the controlling factors. Climate and hydrological data from 224 hydrological stations and 247 meteorological stations in the middle and lower reaches of the Yangtze River basin was analyzed, along with the modeled soil moisture. Except the regulated watersheds, the relative importance of antecedent soil moisture and daily rainfall present significant correlation with drainage area: the larger the watershed is, the more essential antecedent soil saturation rate is in flood generation, the less important daily rainfall is.

Using the percentile of antecedent soil moisture and rainfall as coordinates, the flood generation mechanism(s) of study watersheds could be grouped into three classes: antecedent soil moisture dominated large flat watersheds, heavy rainfall dominated steep and small to middle size watersheds, and small to middle size watersheds with gentle topographic gradient where floods occurrence requires both highly saturated soil and heavy rainfall. Our analysis further shows that the ratio of relative importance between antecedent soil moisture and rainfall (SPR) can be predicted by topographic wetness index. When the topographic wetness index is large, the dominance of antecedent soil moisture for extreme floods is stronger, and *vice versa*. The SPR also

484 presents negative correlation with area normalized flood peak.

485 With the potential increase of extreme rainfall events (Gao et al., 2016; Chen et
486 al., 2016), upstream mountainous watersheds in the middle and lower Yangtze River
487 basin are facing higher risk of extreme floods. The lack of hydrological records further
488 increases the vulnerability of people in these watersheds. The flood risks could be
489 reduced by construction of flood control facilities, but it is difficult to set flood control
490 standards in these ungauged watersheds. Our findings provide a framework to
491 quantitatively estimate the possible flood risk for these ungauged watersheds. Based on
492 measurable watershed characteristics (i.e., drainage area and topographic gradient), the
493 flood generation SPR could be derived, which could then be used to estimate the mean
494 annual flood. This information can provide scientific support for flood control
495 management as well as infrastructures construction.

496 Future analysis at event scale could help generate the flood-generation curve
497 between SPR and discharge at event scale to further improve flood risk predictions in
498 these small ungauged watersheds. With more data from other regions and improved
499 estimation or observation of soil moisture, we could expand our analysis to watersheds
500 with more diverse climate and topographic characteristics to examine and refine our
501 findings and to enhance our understandings of flood generation.

502

503 **Data availability**

504 DEM data was downloaded from Geospatial Data Cloud at http://www.gscloud.cn/.
505 Climatological data used in this study was obtained from China Meteorological Data
506 Network, which can be accessed at http://data.cma.cn/. Discharge data comes from
507 Annual Hydrological Report of the People's Republic of China issued by Yangtze River
508 Water Resources Commission.

509

Acknowledgements

This research was funded by the National Key Research and Development Program of China (2019YFC1510701-01), and National Natural Science Foundation of China (51979243).

References

Abbas, S.A., Xuan, Y. and Song, X.: Quantile Regression Based Methods for Investigating Rainfall Trends Associated with Flooding and Drought Conditions. Water Resources Management, 33(12), 4249-4264, https://doi:10.1007/s11269-019-02362-0, 2019.

Alfonso R., Nilza M. R.C., and Anderson L. R.: Numerical Modelling of the Topographic Wetness Index: An Analysis at Different Scales, International Journal of Geosciences(4), 476-483, https:// doi:10.4236/ijg.2011.24050, 2011.

Allen R. G., Pereira L. S. and Races D.: Crop evapotranspiration-Guidelines for computing crop water requirements FAO Irrigation and drainage paper NO.56(Electric Publication)[M], Rome , Italy:FAO, 1998.

Bennett, B., Leonard, M., Deng, Y., Westra, S.: An empirical investigation into the effect of antecedent precipitation on flood volume. J. Hydrol. 567, 435–445. https://doi.org/10.1016/j.jhydrol.2018.10.025, 2018.

Berghuijs, W.R., Allen, S.T., Harrigan, S. and Kirchner, J.W.: Growing Spatial Scales of Synchronous River Flooding in Europe. Geophysical Research Letters, 46(3), 1423-1428, https://doi:10.1029/2018GL081883, 2019a.

Berghuijs, W.R., Harrigan, S., Molnar, P., Slater, L.J. and Kirchner, J.W.: The Relative Importance of Different Flood-Generating Mechanisms Across Europe. Water Resources Research, 55(6), 4582-4593, https://doi:10.1029/2019WR024841, 2019b.

Berghuijs, W.R., Woods, R.A., Hutton, C.J. and Sivapalan, M.: Dominant flood generating mechanisms across the United States. Geophysical Research Letters, 43(9), 4382-4390, https://doi:10.1002/2016GL068070, 2016.

Bertola, M., Viglione, A., Vorogushyn, S., Lun, D., Merz, B., Blöschl, G.: Do small and large floods have the same drivers of change? A regional attribution analysis in Europe. Hydrol. Earth Syst. Sci. 25, 1347–1364. https://doi.org/10.5194/hess-25-1347-2021, 2021.

543 Bloschl, G., Nester, T., Komma, J., Parajka, J. and Perdigao, R.A.P.: The June 2013
544 flood in the Upper Danube Basin, and comparisons with the 2002, 1954, and 1899
545 floods. Hydrol. Earth Syst. Sci., 17, 5197–5212, 2013.

546 Blöschl, G., Hall, J., Parajka, J., Perdigão, R. A., Merz, B., Arheimer, B., et al.:
547 Changing climate shifts timing of European floods. Science, 357(6351), 588–
548 590. https://doi.org/10.1126/science.aan2506, 2017.

549 Bloschl, G., Hall, J., Viglione, A., Perdigao, R.A., Parajka, J., Merz, B., et al.: Changing
550 climate both increases and decreases European river floods, Nature, 573, 108 –
551 111, 2019.
552 Berti, A., Tardivo, G., Chiaudani, A., Rech, F. and Borin, M.: Assessing reference
553 evapotranspiration by the Hargreaves method in north-eastern Italy. Agricultural
554 Water Management, 140, 20-25, https://doi:10.1016/j.agwat.2014.03.015, 2014.

555 Brunner, M. I., Seibert, J. and Favre, A.C.: Bivariate return periods and their importance
556 for flood peak and volume estimation. Wire's Water, 3, 819 – 833.
557 https://doi.org/10.1002/wat2.1173, 2016.

558 Brunner, M. I., Gilleland, E., Wood, A., Swain, D. L., and Clark, M.: Spatial
559 dependence of floods shaped by spatiotemporal variations in meteorological and
560 land - surface processes. Geophysical Research Letters, 47, e2020GL088000.
561 https://doi.org/ 10.1029/2020GL088000, 2020.

562 Brunner, M. I., Swain, D. L., Wood, R.R. et al. An extremeness threshold determines
563 the regional response of floods to changes in rainfall extremes. Commun Earth
564 Environ 2, 173. https://doi.org/10.1038/s43247-021-00248-x, 2021.

565 Cai, Q. H.: Great protection of Yangtze River and watershed ecology, Yangtze River
566 (01), 70-74, https://doi:10.16232/j.cnki.1001-4179.2020.01.011, 2020.

567 Cen, S.-x., Gong, Y.-f., Lai, X. and Peng, L.: The Relationship between the
568 Atmospheric Heating Source/Sink Anomalies of Asian Monsoon and

569 Flood/Drought in the Yangtze River Basin in the Meiyu Period. Journal of
570 Tropical Meteorology, 21(4), 352-360, 2015.
571 Che, Q., Su, X., Zheng, S., Li, Y.: Interaction between surface water and groundwater
572 in the Alluvial Plain (anqing section) of the lower Yangtze River Basin:
573 environmental isotope evidence. Journal of Radioanalytical and Nuclear
574 Chemistry, 329, 1331–1343, 2021.
575 Chen, Y. and Zhai, P.: Mechanisms for concurrent low-latitude circulation anomalies
576 responsible for persistent extreme precipitation in the Yangtze River Valley.
577 Climate Dynamics,47(3-4), 989-1006, https://doi:10.1007/s00382-015-2885-6,
578 2016.
579 CRED (2015). The human cost of natural disasters: A gobal perspective: Centre for
580 research on the epidemiology of disasters.
581 Deb, P., Kiem, A.S. and Willgoose, G.: Mechanisms influencing non-stationarity in
582 rainfall-runoff relationships in southeast Australia. Journal of Hydrology, 571,
583 749-764, https://doi:10.1016/j.jhydrol.2019.02.025, 2019.

584 Desai, B., Maskrey, A., Peduzzi, P., De Bono, A., & Herold, C. Making Development
585 Sustainable: The Future of Disaster Risk Management. Global Assessment Report
586 on Disaster Risk Reduction http://archive-ouverte.unige.ch/unige:78299 (UNISDR,
587 2015).

588 Do, H. X., Mei, Y., & Gronewold, A. D.: To what extent are changes in flood magnitude
589 related to changes in precipitation extremes? Geophysical Research Letters, 47,
590 e2020GL088684. https://doi.org/10.1029/2020GL088684, 2020.

591 Fang, X. and Pomeroy, J.W.: Impact of antecedent conditions on simulations of a flood
592 in a mountain headwater basin. Hydrological Processes, 30(16), 2754-2772,
593 https://doi:10.1002/hyp.10910, 2016.
594 Feng, B. F., Dai M. L. and Zhang T.: Effect of Reservoir Group Joint Operation on
595 Flood Control in the Middle and Lower Reaches of Yangtze River, Journal of
596 Water Resources Research (3), 278-284, https://doi:10.12677/JWRR.2017.63033,
597 2017.
598 Fu, G., Yu, J., Yu, X., Ouyang, R., Zhang, Y., Wang, P., Liu, W. and Min, L.: Temporal
599 variation of extreme rainfall events in China, 1961-2009. Journal of Hydrology,
600 487, 48-59, https://doi:10.1016/j.jhydrol.2013.02.021, 2013.

601 Gao, T. and Xie, L.: Spatiotemporal changes in precipitation extremes over Yangtze
602 River basin, China, considering the rainfall shift in the late 1970s. Global and
603 Planetary Change, 147, 106-124, https://doi:10.1016/j.gloplacha.2016.10.016,
604 2016.
605 Gao, Y., Wang, H., Lu, X., Xu, Y., Zhang, Z. and Schmidt, A.R.: Hydrologic Impact
606 of Urbanization on Catchment and River System Downstream from Taihu Lake.
607 Journal of Coastal Research, 82-88, https://doi:10.2112/SI84-012.1, 2018.
608 Garg, S., & Mishra, V.: Role of extreme precipitation and initial hydrologic conditions
609 on floods in Godavari river basin, India. Water Resources Research, 55, 9191–
610 9210. https://doi.org/10.1029/2019WR025863, 2019.
611 Grabs, T., Seibert, J., Bishop, K. and Laudon, H.: Modeling spatial patterns of saturated
612 areas: A comparison of the topographic wetness index and a dynamic distributed
613 model. Journal of Hydrology, 373(1-2), 15-23,
614 https://doi:10.1016/j.jhydrol.2009.03.031, 2009.
615 Huang, C., Zhou, Y., Zhang, S., Wang, J., Liu, F., Gong, C., Yi, C., Li, L., Zhou, H.,
616 Wei, L., Pan, X., Shao, C., Li, Y., Han, W., Yin, Z., and Li, X.: Groundwater
617 resources in the Yangtze River Basin and its current development and utilization[J].
618 Geology of China, 2021, 48(4):979-1000.
619 IPCC. Managing the Risks of Extreme Events and Disasters to Advance Climate
620 Change Adaptation (eds Field, C. B. et al.) (Cambridge Univ. Press, 2012).
621 Kato, K.: On the Abrupt Change in the Structure of the Baiu Front over the China
622 Continent in Late May of 1979. Journal of the Meteorological Society of Japan,
623 63(1), 20-36, https://doi:10.2151/jmsj1965.63.1_20, 1985.
624 Kazuki, T., Oliver C. S. V., Masahiro, R.: Spatial variability of precipitation and soil
625 moisture on the 2011 flood at chao phraya river basin.International Water
626 Technology Association, Proceedings of Hydrology and Water Resources, B, 17-
627 21, 2013.
628 Kemter, M., Merz, B., Marwan, N., Vorogushyn, S., & Blöschl, G.: Joint trends in flood
629 magnitudes and spatial extents across Europe. Geophysical Research Letters, 47,
630 e2020GL087464. https://doi.org/10.1029/2020GL087464, 2020.
631 Lehner, B., C. Reidy Liermann, C. Revenga, C. Vörösmarty, B. Fekete, P. Crouzet, P.
632 Döll, M. Endejan, K. Frenken, J. Magome, C. Nilsson, J.C. Robertson, R. Rodel,
633 N. Sindorf, and D. Wisser. 2011. High-resolution mapping of the world's

reservoirs and dams for sustainable river-flow management. Frontiers in Ecology and the Environment 9 (9): 494-502.

Li, Q., Wei, F. and Li, D.: Interdecadal variation of East Asian summer monsoon and drought/flood distribution over eastern China in the last 159 years. Journal of Geographical Sciences, 21(4), 579-593, https://doi:10.1007/s11442-011-0865-2, 2011.

Li, X., Zhang, K., Gu, P., Feng, H., Yin, Y., Chen, W. and Cheng, B.: Changes in precipitation extremes in the Yangtze River Basin during 1960-2019 and the association with global warming, ENSO, and local effects. Science of the Total Environment, 760, https://doi:10.1016/j.scitotenv.2020.144244, 2021.

Liu, B., Yan, Y., Zhu, C., Ma, S., & Li, J.: Record-breaking Meiyu rainfall around the Yangtze River in 2020 regulated by the subseasonal phase transition of the North Atlantic Oscillation. Geophysical Research Letters, 47, e2020GL090342. https://doi. Org/10.1029/2020GL090342, 2020.

Liu, L., Ye, S., Chen, C., Pan, H. and Ran, Q.: Nonsequential Response in Mountainous Areas of Southwest China. Frontiers in Earth Science, 9: 1-15. doi: 10.3389/feart.2021.660244, 2021

Liu, N., Jin, Y. and Dai, J.: Variation of Temperature and Precipitation in Urban Agglomeration and Prevention Suggestion of Waterlogging in Middle and Lower Reaches of Yangtze River. 3rd International Conference on Energy Equipment Science and Engineering (Iceese 2017), 128, https://doi:10.1088/1755-1315/128/1/012165, 2018.

Liu, S., Huang, S., Xie, Y., Wang, H., Leng, G., Huang, Q., Wei, X., and Wang, L.: Identification of the Non-stationarity of Floods: Changing Patterns, Causes, and Implications, Water Resour. Manag., 33, 939–953, 2018.

Liu, Y., Xinyu, L., Liancheng, Z., Yang, L., Chunrong, J., Ni, W. and Juan, Z.: Quantifying rain, snow and glacier meltwater in river discharge during flood events in the Manas River Basin, China. Natural Hazards, 108(1), 1137-1158, https://doi:10.1007/s11069-021-04723-8, 2021.

Long, L.H., Ji, D.B., Yang, Z.Y., Cheng, H.Q., Yang, Z.J., Liu, D.F., Liu, L. and Lorke, A.: Tributary oscillations generated by diurnal discharge regulation in Three Gorges Reservoir. Environmental Research Letters, 15(8), https://doi:10.1088/1748-9326/ab8d80, 2020.

Lu, M., Wu, S.-J., Chen, J., Chen, C., Wen, Z. and Huang, Y.: Changes in extreme precipitation in the Yangtze River basin and its association with global mean temperature and ENSO. International Journal of Climatology, 38(4), 1989-2005, https://doi:10.1002/joc.5311, 2018.

Meles, M.B., Younger, S.E., Jackson, C.R., Du, E., Drover, D.: Wetness index based on landscape position and topography (WILT): Modifying TWI to reflect landscape position, Journal of Environmental Management 255, 109863, 2020.

Miao, Q., Huang, M. and Li, R., Q.: Response of net primary productivity of vegetation in Yangtze River Basin to future climate change. Journal of Natural Resources, 25, 08(2010):1296-1305, doi:CNKI:SUN:ZRZX.0.2010-08-007, 2015.

Munoz, S.E., Giosan, L., Therrell, M.D., Remo, J.W.F., Shen, Z., Sullivan, R.M., Wiman, C., O'Donnell, M., and Donnelly, J.P.: Climatic control of Mississippi River flood hazard amplified by river engineering, 556, 95 – 98, 2018.

Musselman, K.N., Lehner, F., Ikeda, K., Clark, M.P., Prein, A.F., Liu, C., Barlage, M. and Rasmussen, R.: Projected increases and shifts in rain-on-snow flood risk over western North America, Nature Climate Change, 8, 808 – 812, 2018.

Ockert J. G. and Jeff C. S.: Review of methods used to estimate catchment response time for the purpose of peak discharge estimation, Hydrological Sciences Journal, 59:11, 1935-1971, DOI: 10.1080/02626667.2013.866712, 2014.

Ohmura, A. and Wild, M.: Is the hydrological cycle accelerating? Science, 298, 1345–1346, 2002.

Pegram, G. and Bardossy, A.: Downscaling Regional Circulation Model rainfall to gauge sites using recorrelation and circulation pattern dependent quantile-quantile transforms for quantifying climate change. Journal of Hydrology, 504, 142-159, https://doi:10.1016/j.jhydrol.2013.09.014, 2013.

Peng, T., Tian, H., Singh, V. P., Chen, M., Liu, J., Ma, H. B. and Wang, J. B.: Quantitative assessment of drivers of sediment load reduction in the Yangtze River basin, China, Journal of Hydrology, 580, https://doi:10.1016/j.jhydrol.2019.124242, 2020.

Qian, H. and Xu, S.-B.: Prediction of Autumn Precipitation over the Middle and Lower Reaches of the Yangtze River Basin Based on Climate Indices. Climate, 8(4), https://doi:10.3390/cli8040053, 2020.

699 Ran, Q., Chen, X., Hong Y., Ye S., and Gao J.: Impacts of terracing on hydrological
700 processes: A case study from the Loess Plateau of China. Journal of Hydrology,
701 588, https:// doi:10.1016/j.jhydrol.2020.125045, 2020.
702 Ran, Q., Zong, X., Ye, S., Gao, J. and Hong, Y.: Dominant mechanism for annual
703 maximum flood and sediment events generation in the Yellow River basin. Catena,
704 187, https://doi:10.1016/j.catena.2019.104376, 2020.
705 Ray S. M., Ramakar J. and Kishanjit K. K.: Precipitation-runoff simulation for a
706 Himalayan River Basin, India using artificial neural network algorithms, Sciences
707 in Cold and Arid Regions, 5(1), 85-95, 2013.
708 Rottler, E., Francke, T., Burger, G., and Bronstert, A.: Long-term changes in central
709 European river discharge for 1869–2016: impact of changing snow covers,
710 reservoir constructions and an intensified hydrological cycle, Hydrol. Earth Syst.
711 Sci., 24, 1721–1740, 2020.
712 Smith, J. A., Cox, A. A., Baeck, M. L., Yang, L., and Bates, P.: Strange floods: the
713 upper tail of flood peaks in the United States, Water Resour. Res., 54, 6510–6542,
714 2018.
715 Sorensen, R., Zinko, U., and Seibert, J.: On the calculation of the topographic wetness
716 index: evaluation of different methods based on field observations, Hydrology and
717 Earth System Sciences, 10, 101–112, 2006.
718 Su, Z., Ho, M., Hao, Z., Lall, U., Sun, X., Chen, X. and Yan, L.: The impact of the
719 Three Gorges Dam on summer streamflow in the Yangtze River Basin.
720 Hydrological Processes, 34(3), 705-717, https://doi:10.1002/hyp.13619, 2020.
721 Suresh, S. S., Benefit O., Augustine T., and Trevor P. : Peoples' Perception on the
722 Effects of Floods in the Riverine Areas of Ogbia Local Government Area of
723 Bayelsa State, Nigeria, Knowledge Management, https://doi:10.18848/2327-
724 7998/CGP/v12i02/50793, 2013.
725 Tao, S. Y., Rainstorm in China [M], Beijing: Science Press, 1980.(in Chinese)
726 Tramblay, Y., Villarini, G., El Khalki, E. M., Gründemann, G., & Hughes, D.:
727 Evaluation of the drivers responsible for flooding in Africa. Water Resources
728 Research, 57, e2021WR029595. https://doi. Org/10.1029/2021WR029595, 2021.

729 USBR (United States Bureau of Reclamation), 1973. Design of small dams. 2nd ed.
730 Washington, DC: Water Resources Technical Publications.
731 Vicente-Serrano, S.M., Azorin-Molina, C., Sanchez-Lorenzo, A., Revuelto, J., Lopez-
732 Moreno, J.I., Gonzalez-Hidalgo, J.C., Moran-Tejeda, E. and Espejo, F.: Reference
733 evapotranspiration variability and trends in Spain, 1961-2011. Global and
734 Planetary Change, 121, 26-40, https://doi:10.1016/j.gloplacha.2014.06.005, 2014.
735 Volpi, E., Di Lazzaro, M., Bertola, M., Viglione, A. and Fiori, A.: Reservoir Effects on
736 Flood Peak Discharge at the Catchment Scale. Water Resources Research, 54(11),
737 9623-9636, https://doi:10.1029/2018wr023866, 2018.
738 Wang, H., Zhou, Y., Pang, Y. and Wang, X.: Fluctuation of Cadmium Load on a Tide-
739 Influenced Waterfront Lake in the Middle-Lower Reaches of the Yangtze River.
740 Clean-Soil Air Water, 42(10), 1402-1408, https://doi:10.1002/clen.201300693,
741 2014.
742 Wang, J., Ran, Q., Liu, L., Pan, H. and Ye, S.: Study on the Dominant Mechanism of
743 Extreme Flow Events in the Middle and Lower Reaches of the Yangtze River,
744 China Rural Water and Hydropower, Accepted.
745 Wang, R., Yao, Z., Liu, Z., Wu, S., Jiang, L. and Wang, L.: Snow cover variability and
746 snowmelt in a high-altitude ungauged catchment. Hydrological Processes, 29(17),
747 3665-3676, https://doi:10.1002/hyp.10472, 2015.
748 Wang, W., Xing W., Yang, T., Shao, Q., Peng, S., Yu, Z., and Yong, B.: Characterizing
749 the changing behaviours of precipitation concentration in the Yangtze River Basin,
750 China. Hydrological Processes, 27(24), 3375-3393, https://doi: 10.1002/hyp.9430,
751 2013.
752 Wang, Z. and Plate, E.: Recent flood disasters in China. Proceedings of the Institution
753 of Civil Engineers – Water and Maritime Engineering (3),
754 https://doi:10.1680/wame.2002.154.3.177, 2002.
755 Wasko, C. and Nathan, R.: Influence of changes in rainfall and soil moisture on trends
756 in flooding. Journal of Hydrology, 575, 432-441,
757 https://doi:10.1016/j.jhydrol.2019.05.054, 2019.
758 Wasko, C., Nathan, R., & Peel, M. C.: Changes in antecedent soil moisture modulate
759 flood seasonality in a changing climate. Water Resources Research, 56,
760 e2019WR026300. https:// doi.org/10.1029/2019WR026300, 2020.

Wasko, C., Nathan, R., Stein, L., O'Shea, D.: Evidence of shorter more extreme rainfalls and increased flood variability under climate change. J. Hydrol. 603, 126994. https://doi.org/10.1016/j.jhydrol.2021.126994, 2021.

Wu, X. S., Guo, S. L. and Ba, H. H.: Long-term precipitation forecast method based on SST multipole index, Journal of water conservancy(10), 1276-1283, https://doi:10.13243/j.cnki.slxb.20180544, 2018.

Xia, J. and Chen, J.: A new era of flood control strategies from the perspective of managing the 2020 Yangtze River flood. Science China-Earth Sciences, 64(1), 1-9, https://doi:10.1007/s11430-020-9699-8, 2021.

Xie, Z., Du, Y., Zeng, Y. and Miao, Q.: Classification of yearly extreme precipitation events and associated flood risk in the Yangtze-Huaihe River Valley. Science China-Earth Sciences, 61(9), 1341-1356, https://doi:10.1007/s11430-017-9212-8, 2018.

Yang, H.F., Yang, S.L., Xu, K.H., Milliman, J.D., Wang, H., Yang, Z., Chen, Z. and Zhang, C.Y.: Human impacts on sediment in the Yangtze River: A review and new perspectives. Global and Planetary Change, 162, 8-17, https://doi:10.1016/j.gloplacha.2018.01.001, 2018.

Yang, L., Wang, L., Li, X. and Gao, J.: On the flood peak distributions over China. Hydrology and Earth System Sciences, 23(12), 5133-5149, https://doi:10.5194/hess-23-5133-2019, 2019.

Yang, W., Yang, H., and Yang, D.: Classifying floods by quantifying driver contributions in the Eastern Monsoon Region of China, Journal of Hydrology, 585, 124767, 2020.

Yang, W., Yang, H., Yang, D., and Hou, A.: Causal effects of dams and land cover changes on flood changes in mainland China. Hydrol. Earth Syst. Sci., 25, 2705–2720, 2021.

Ye, S., Li, H., Leung, L.R., Guo, J., Ran, Q., Demissie, Y., et al., 2017. Understanding flood seasonality and its temporal shifts within the contiguous United States. J. Hydrometeorol. 18 (7), 1997–2009.

Ye, X., Xu, C.-Y., Li, Y., Li, X. and Zhang, Q.: Change of annual extreme water levels and correlation with river discharges in the middle-lower Yangtze River: Characteristics and possible affecting factors. Chinese Geographical Science,27(2), 325-336, https://doi:10.1007/s11769-017-0866-x, 2017.

794 Yu, F., Chen, Z., Ren, X. and Yang, G.: Analysis of historical floods on the Yangtze
795 River, China: Characteristics and explanations. Geomorphology,113(3-4), 210-
796 216, https://doi:10.1016/j.geomorph.2009.03.008, 2009.
797 Zaherpour, J., Gosling, S. N., Mount, N., Schmied, H. M., Veldkamp, T. I., et
798 al. :Worldwide evaluation of mean and extreme runoff from six global-scale
799 hydrological models that account for human impacts. Environmental Research
800 Letters, 13(6), 065015. https://doi. org/10.1088/1748-9326/aac547, 2018.
801 Zhang, H., Liu, S., Ye, J. and Yeh, P.J.F.: Model simulations of potential contribution
802 of the proposed Huangpu Gate to flood control in the Lake Taihu basin of China.
803 Hydrology and Earth System Sciences, 21(10), 5339-5355,
804 https://doi:10.5194/hess-21-5339-2017, 2017.
805 Zhao, J., Li, J., Yan, H., Zheng, L. and Dai, Z.: Analysis on the Water Exchange
806 between the Main Stream of the Yangtze River and the Poyang Lake. 2011 3rd
807 International Conference on Environmental Science and Information Application
808 Technology Esiat 2011, Vol 10, Pt C,10, 2256-2264,
809 https://doi:10.1016/j.proenv.2011.09.353, 2011.
810 Zhang, S., Kang, L. and He, X.: Equal proportion flood retention strategy for the leading
811 multireservoir system in upper Yangtze River. International Conference on Water
812 Resources and Environment, WRE 2015, 2015.
813 Zhang, W., Villarini, G., Vecchi, G.A. and Smith, J. A.: Urbanization exacerbated the
814 rainfall and flooding caused by hurricane Harvey in Houston. Nature, 563, 384 –
815 388, 2018.
816 Zhang, K., Wang, Q., Chao, L., Ye, J., Li, Z., Yu, Z., Yang, T. and Ju, Q.: Ground
817 observation-based analysis of soil moisture spatiotemporal variability across a
818 humid to semi-humid transitional zone in China. Journal of Hydrology, 574, 903-
819 914, 2019.
820 Zou, B., Li, Y., Feng, B.: Analysis on dispatching influence of Three Gorges Reservoir
821 on water level of main stream in mid-lower reaches of Yangtze River: a case study
822 of flood in July,2010. Yangtze River, 42.06:80-82+100. doi:10.16232/j.cnki.1001-
823 4179.2011.06.004, 2011.
824
825

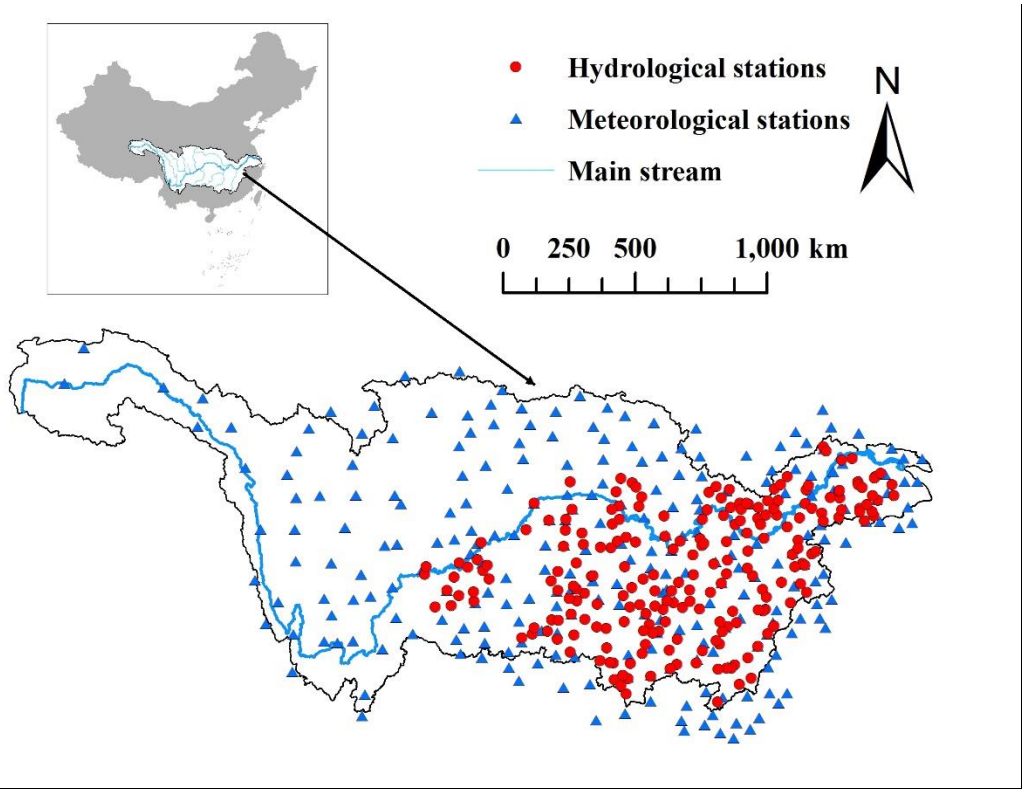

826

827 **Figure 1**: Map of the Yangtze River basin, and the meteorological stations and
828 hydrological stations. The blue line is the main stream of Yangtze River.

829

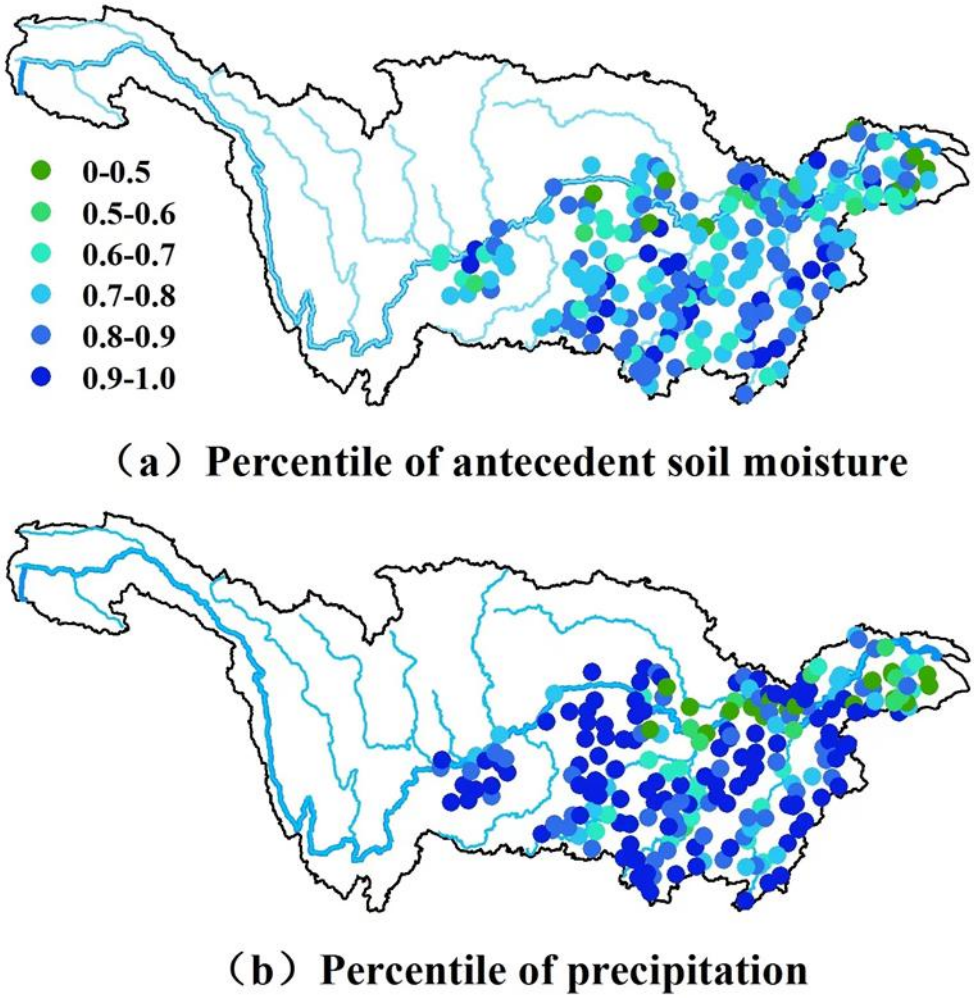

Figure 2: The spatial distribution of (a) the percentile of antecedent soil moisture during annual maximum flood; (b) the percentile of daily precipitation during annual maximum flood.

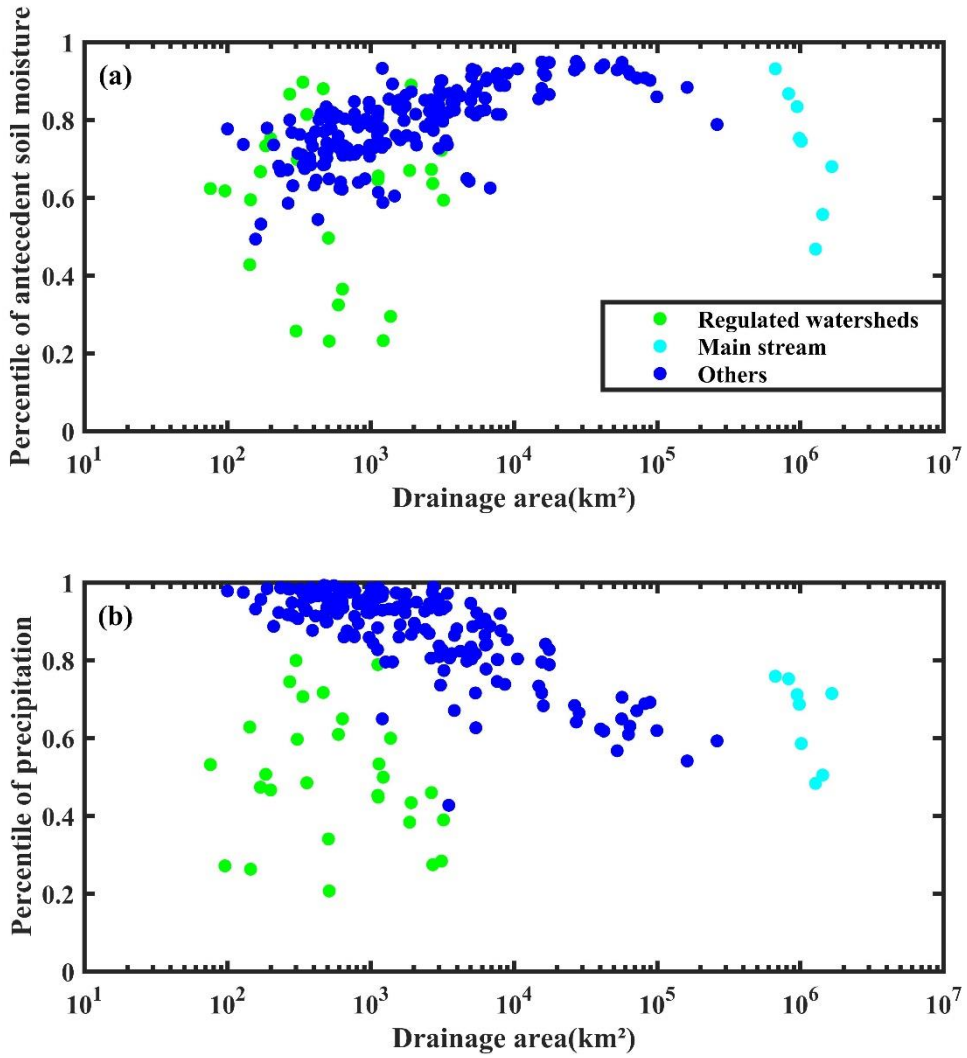

835

836 **Figure 3**: Scatterplot between the drainage area and (a) the percentile of antecedent soil
837 moisture of AMF events (the linear regression for blue dots: $R^2 = 0.46$, p-value<0.001);
838 (b) the percentile of precipitation at the day of AMF events (the linear regression for
839 blue dots: $R^2 = 0.61$, p-value<0.001). The green dots represent the regulated watershed,
840 the cyan dots represent the sites on the main stream, and the rest sites are shown in blue.

841

842

843

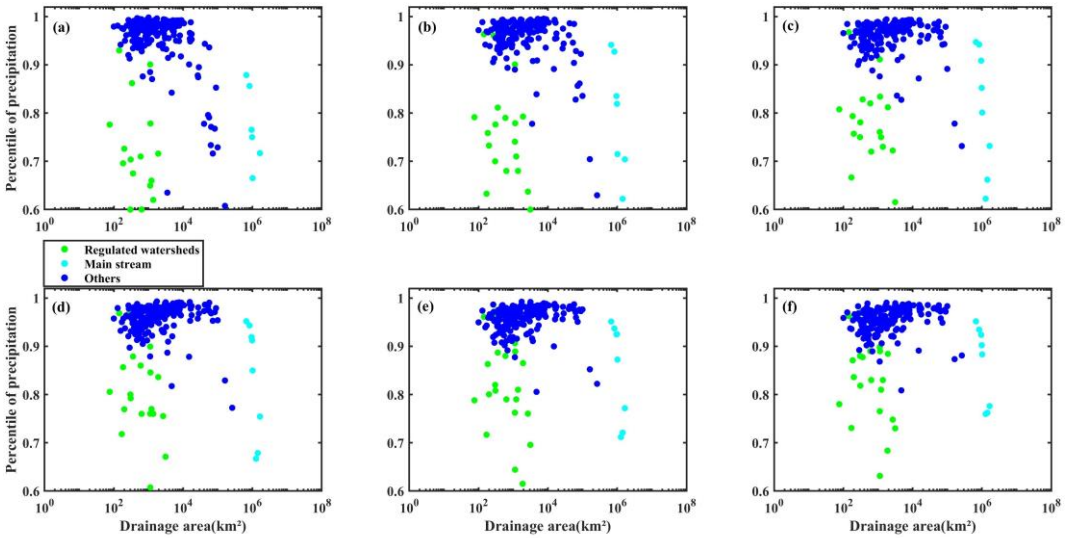

844

845 **Figure 4**: Scatterplot between the drainage area and the percentile of accumulated
846 rainfall of (a) two days; (b) three days; (c) four days; (d) five days; (e) six days; and (f)
847 seven days on AMF events.

848

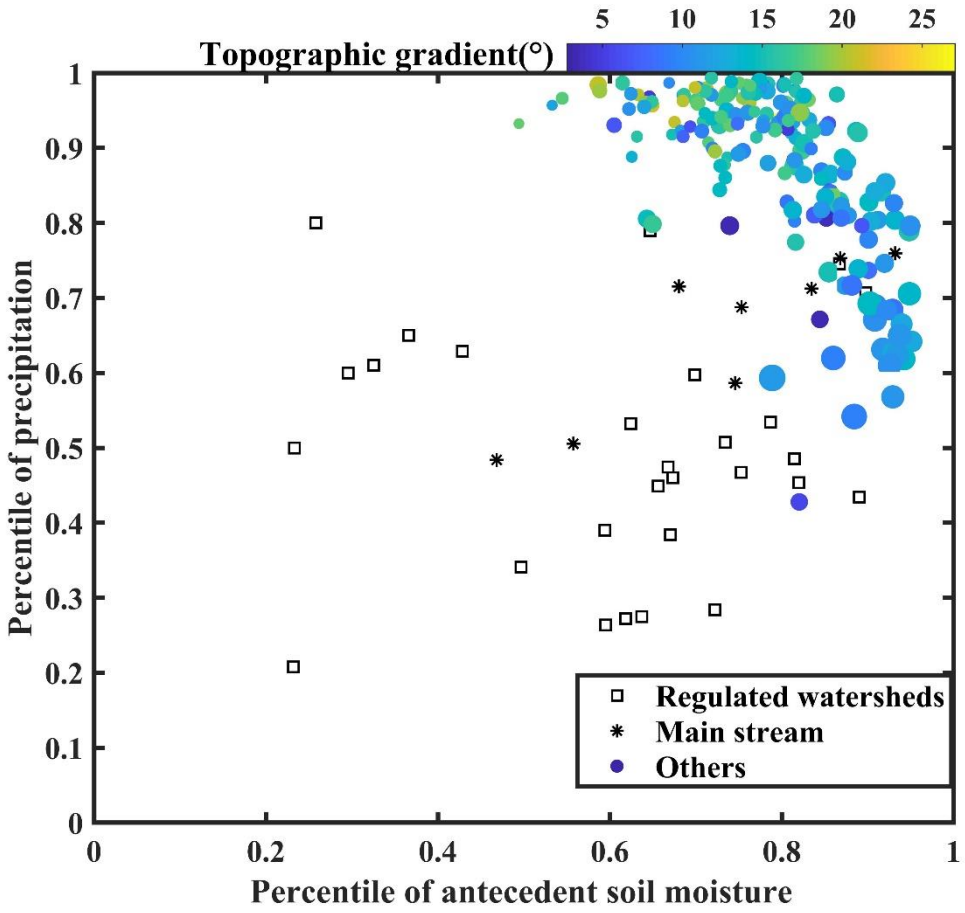

Figure 5: Scatterplot of the percentile of precipitation and antecedent soil moisture, the color represents topographic gradient and the size of circles is scaled by drainage area.

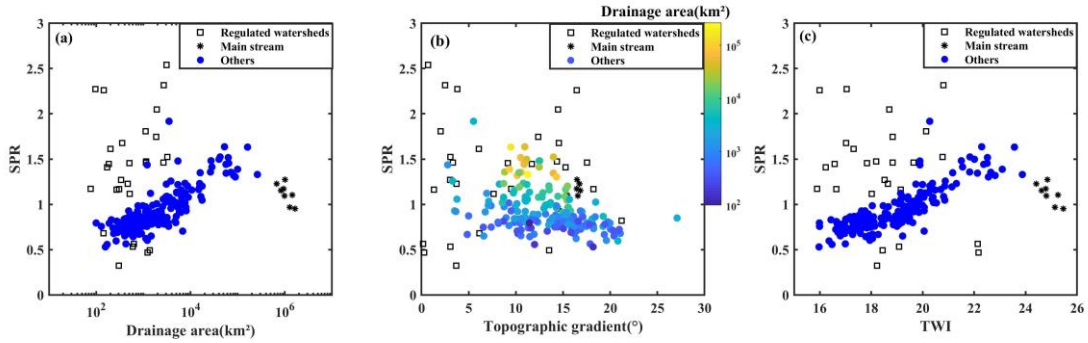

Figure 6: Scatterplots between the ratio of antecedent soil moisture and precipitation (SPR) and (a) drainage area; (b) slope; and (c) topographic wetness index (TWI).

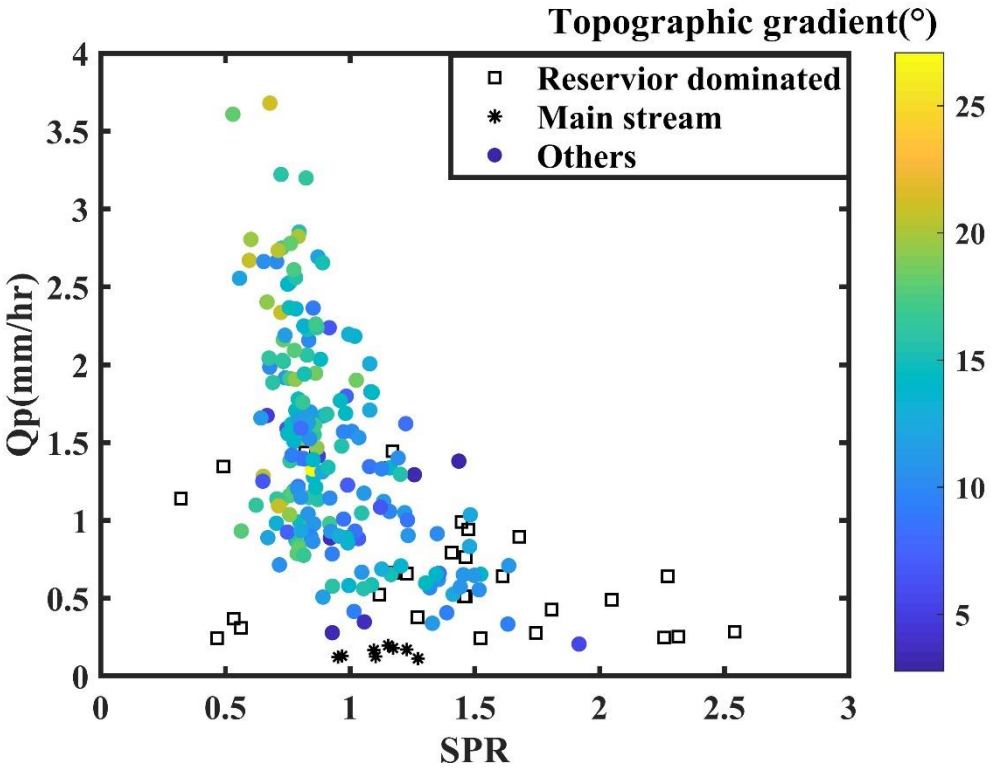

Figure 7: Scatterplot between the ratio of antecedent soil moisture and precipitation (SPR) and area weighted annual maximum discharge (Q_P), the color represents topographic gradient.

Supplementary

Table S1: Estimated concentration time for 10 sites with largest drainage area: the ones on main stream (MS) and the ones at the outlets of major tributaries (TR).

Site Name	Concentration Time (hr)	Drainage Area (km²)
TR-Hukou	17.9	161,979
TR-Chenglingji	18.8	261,986
MS-Zhutuo	32.7	668,661
MS-Cuntan	32.8	827,799
MS-Wanxian	37.6	948,524
MS-Yichang	41.5	982,948
MS-Jianli	45.2	1,014,690
MS-Luoshan	46.3	1,276,676
MS-Hankou	51.0	1,432,008
MS-Datong	54.3	1,657,604

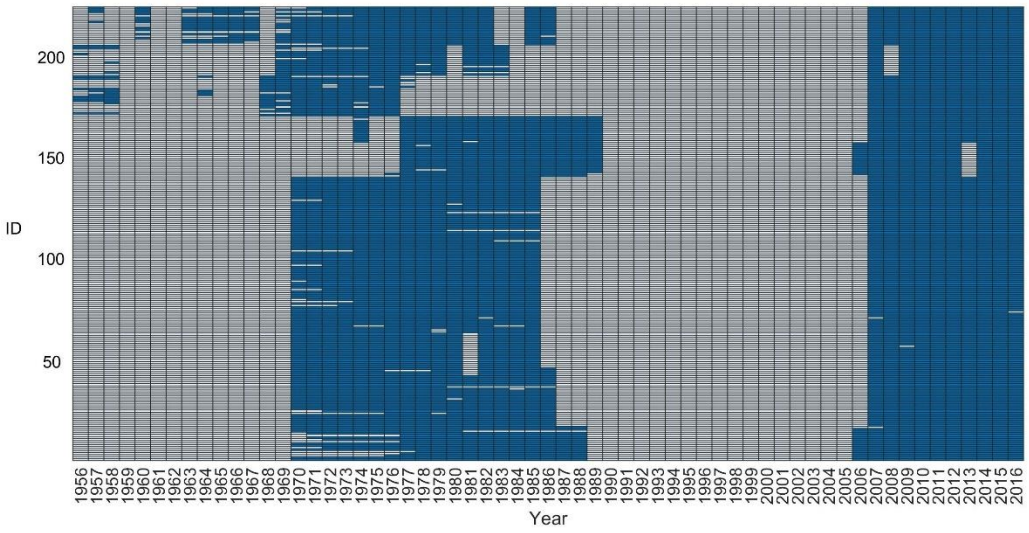

872

873 **Figure S1**: The data availability of each station, each column indicates each year while

874 each row is corresponding to each station, blue grid indicates there is record of this year.